A facile route to inverted polymer solar cells using a precursor based zinc oxide electron transport layer

de Bruyn, P.; Moet, D. J. D.; Blom, P. W. M.

Published in:
Organic Electronics

DOI:
10.1016/j.orgel.2010.06.002

Publication date:
2010

Organic Electronics 11 (2010) 1419–1422

Contents lists available at ScienceDirect

Organic Electronics

journal homepage: www.elsevier.com/locate/orgel

Letter

A facile route to inverted polymer solar cells using a precursor based zinc oxide electron transport layer

P. de Bruyn [a,b,*], D.J.D. Moet [a], P.W.M. Blom [a,c]

[a] Molecular Electronics, Zernike Institute for Advanced Materials, University of Groningen, Nijenborgh 4, 9747 AG Groningen, The Netherlands
[b] Dutch Polymer Institute, 5600 AX Eindhoven, The Netherlands
[c] Holst Centre, High Tech Campus 31, 5605 KN Eindhoven, The Netherlands

ARTICLE INFO

Article history:
Received 15 March 2010
Received in revised form 4 June 2010
Accepted 5 June 2010
Available online 17 June 2010

Keywords:
Polymer
Organic
Solar cell
Inverted
Zinc oxide
Zinc acetylacetonate

ABSTRACT

Inverted polymer:fullerene solar cells with ZnO and MoO_3 transport layers are demonstrated. ZnO films are prepared through spin casting of a zinc acetylacetonate hydrate solution, followed by low temperature annealing under ambient conditions. The performance of solar cells with an inverted structure is shown to be equivalent to that of conventional cells with a bottom-anode–top-cathode configuration for three efficient polymer:fullerene systems.

1. Introduction

Due to concentrated efforts to increase organic photovoltaic device performance in recent years, confirmed power conversion efficiencies have currently exceeded 7% [1,2]. However, one of the drawbacks of solar cells based on polymers is the use of poly(3,4-ethylene dioxythiophene) (PEDOT) doped with poly(4-styrenesulfonate) (PSS), since the ITO/PEDOT:PSS interface is not stable and has an adverse affect on organic device performance over time [3,4]. Inverted devices utilizing an evaporated metal oxide/metal anode (e.g. MoO_3/Al) instead of PEDOT:PSS have shown comparable performance to their conventional counterparts [5–8]. Furthermore, zinc oxide (ZnO) has successfully been applied as a low work function cathode in inverted solar cell structures [9–11], organic tandem solar cell devices [12], and even as acceptor material in polymer:ZnO bulk heterojunctions [13–15]. In the nanoparticle approach, ZnO nanoparticles (nc-ZnO) of approximately 5 nm in diameter were synthesized by hydrolysis and condensation of zinc acetate dihydrate by KOH in methanol, using the method of Pacholski et al. [16]. Furthermore, MoO_3 has been used in organic light emitting diodes as the anode material in several studies [17–21]. To further simplify the processing and exclude the nanoparticle synthesis, we introduce a simple, low temperature solution process to fabricate ZnO films for electronic devices. This alternative process for the ZnO cathode involves spin casting and subsequent pyrolysis of the precursor material zinc acetylacetonate ($Zn(acac)_2$) hydrate. This material has been shown to react with H_2O to form ZnO at low temperatures and high humidity conditions in metal–organic chemical vapor deposition (MOCVD) experiments [22]. The proposed mechanism for such a low temperature decomposition is that the high humidity conditions prevent dehydration of the hydrated material and enable a single step conversion of the precursor to ZnO at temperatures below 120 °C, making the process compatible with a

* Corresponding author at: Molecular Electronics, Zernike Institute for Advanced Materials, University of Groningen, Nijenborgh 4, 9747 AG Groningen, The Netherlands. Tel.: +31 50 363 4866.
E-mail address: p.de.bruyn@rug.nl (P. de Bruyn).

1566-1199/$ - see front matter © 2010 Elsevier B.V. All rights reserved.
doi:10.1016/j.orgel.2010.06.002

large amount of organic materials and devices. We demonstrate inverted solar cells with precursor ZnO electron transport layers for three well-studied polymer:fullerene systems, i.e. based on poly(3-hexylthiophene) (P3HT), poly[9,9-didecanefluorene-*alt*-(bis-thienylene) benzothiadiazole] (PF10TBT) and poly[2,6-(4,4-bis-(2-ethylhexyl)-4H-cyclopenta[2,1-*b*;3,4-*b*′]dithiophene)-*alt*-4,7-(2,1,3-benzothiadiazole)] (PCPDTBT). As an acceptor the standard [6,6]-phenyl-C_{61}-butyric acid methyl ester (PCBM) has been used. All three blends can provide power conversion efficiencies in excess of 4% in combination with a fullerene acceptor [23–25]. Our inverted solar cell structures using precursor ZnO exhibit a performance that is identical to conventional bottom-anode–top-cathode geometry solar cells.

2. Experimental

Zinc oxide layers were prepared by dissolving 20 mg/mL of $Zn(acac)_2$ hydrate (obtained from Sigma–Aldrich) in absolute ethanol under ambient conditions, stirring for several hours at 50 °C and subsequently filtering with a 0.2 μm pore size PTFE filter. ITO covered glass substrates were cleaned with soap and deionised water, followed by ultrasonic treatment in acetone and 2-isopropanol. Afterwards they were dried in an oven at 140 °C for 10 min in ambient conditions, followed by UV-ozone treatment for 20 min. $Zn(acac)_2$ was spin cast in air at 1000 rpm, while both solution and substrates were held at 50 °C. Hydrolysis of the precursor was carried out in air during 30 s on a hotplate at 120 °C. This generally resulted in a 20 nm thick layer of ZnO. ZnO typically requires UV illumination to transform from an intrinsic semiconductor into an n-type material by desorption of O_2^- radicals from the surface [26,27]. After illumination with a Steuernagel SolarConstant 1200 metal halide lamp, a reduction of the work function from 4.2 to 3.7 eV was measured with a Kelvin probe calibrated to a gold reference. This is in line with the assumption of injection of electrons into the conduction band by UV illumination and a corresponding raise of the Fermi level. P3HT:PCBM (1:0.8 by weight, 15 mg/mL of polymer) was dissolved in chloroform. PCPDTBT:PCBM (1:2.5 by weight, 7 mg/mL of polymer) was dissolved in a chlorobenzene solution containing 1.5 wt.% 1,8-octanedithiol, which was added to increase the photovoltaic performance of the resulting devices as described in literature [23,28]. PF10TBT:PCBM (1:4 by weight, 3 mg/mL of polymer) was dissolved in pristine chlorobenzene. ITO substrates were cleaned as described before. PEDOT:PSS (Clevios P VP AI 4083) was spin cast in air to yield a 50 nm layer on the substrate. Spin casting of the P3HT:PCBM and PCPDTBT:PCBM blends was done in a nitrogen atmosphere, while PF10TBT:PCBM was spin cast in air. Thermal evaporation was performed at a pressure of 10^{-6} mbar for all materials (LiF, Al and MoO_3). MoO_3 powder was obtained from Sigma–Aldrich and was used as received. The evaporation rate was held constant at 0.05 nm/s to produce a smooth film of 10 nm and 1 nm for MoO_3 and LiF, respectively. Finished cells were illuminated through illumination masks with a Steuernagel SolarConstant 1200 metal halide lamp, calibrated to 1 sun intensity and corrected for spectral mismatch with the AM1.5G spectrum using a Si reference cell. The calculated mismatch factors for P3HT:PCBM, PF10TBT:PCBM and PCPDTBT:PCBM in this setup amounted to 1.40, 1.40 and 1.03, respectively [29]. Electrical characterization was done with a Keithley 2400 SourceMeter.

3. Results and discussion

The optical absorbance of a 20 nm layer of ZnO was measured with respect to a glass reference with a Perkin-Elmer Lambda 900 spectrophotometer and is shown in Fig. 1. Note the excellent optical transparency in the visible range of wavelengths of the precursor made ZnO film. The optical absorbance of the precursor layer before conversion is shown for reference. The inset provides a determination of the optical band gap of the ZnO films through extrapolation of the linear regime in the quadratic absorption to 3.53 eV. Furthermore, the structure of $Zn(acac)_2$ is shown for clarity. Fig. 2 shows the structure of the completed cells, along with the materials used for the active layers. The current density–voltage characteristics of the P3HT:PCBM, PF10TBT:PCBM and the PCPDTBT:PCBM cells under illumination are shown in Fig. 3. All photoactive layers were approximately 80 nm thick. Table 1 shows the performance parameters for all solar cells presented in this study. We observe that the performance parameters and thus the cell efficiencies are very close for cells with the conventional and inverted geometry. The reported efficiencies are in good agreement with previously published values for optimized PF10TBT:PCBM cells [24]. The efficiency of the PCPDTBT:PCBM cells has been increased in comparison to a previous publication, which is due to decreased recombination by addition of 1,8-octanedithiol in these devices [28,30]. Furthermore, optical absorption simulations based on the transfer matrix formalism have been performed on the two structures for the PF10TBT:PCBM blend [31–34]. The optical constants needed for this simulation

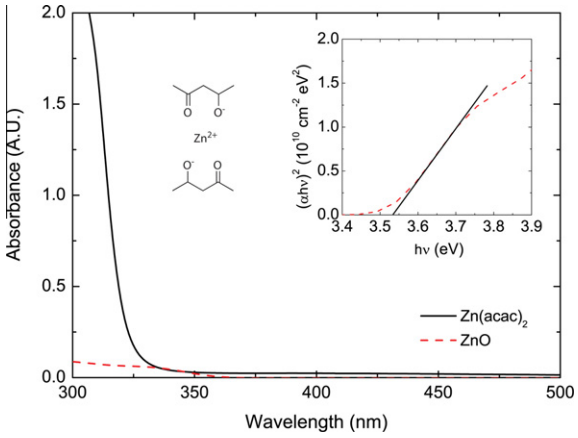

Fig. 1. Optical absorbance of a 20 nm layer of ZnO. The absorbance of the $Zn(acac)_2$ precursor layer is shown for reference. The inset shows the determination of the optical band gap for the ZnO layer. The chemical structure of $Zn(acac)_2$ is shown for clarity.

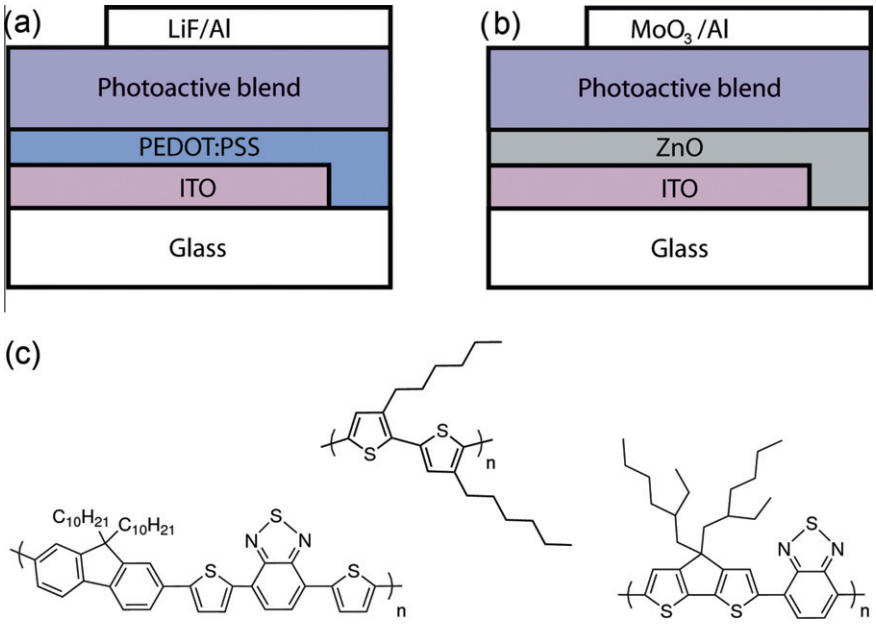

Fig. 2. Solar cell geometries and polymers used in this study. (a) Conventional bottom-anode–top-cathode structure. (b) Inverted bottom-cathode–top-anode structure. (c) Chemical structures of PF10TBT (left), P3HT (middle) and PCPDTBT (right).

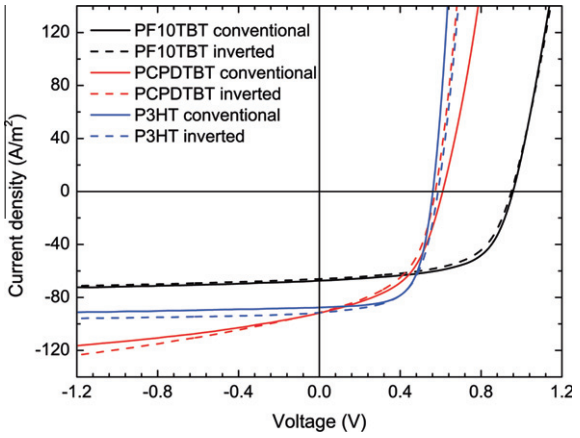

Fig. 3. *J–V* characteristics of solar cells employing both contact geometries for the two material blends. 'Inverted' denotes the bottom-cathode–top-anode structure.

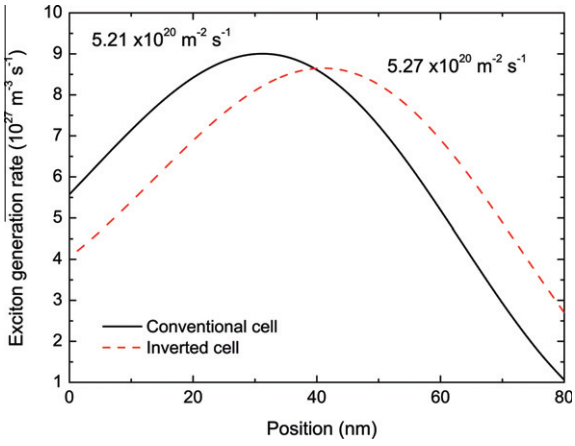

Fig. 4. Simulated exciton generation rates in conventional and inverted geometry cells. The origin is defined as the substrate side of the device. The integrated generation rates are shown for the two geometries.

Table 1
Photovoltaic properties of conventional and inverted PF10TBT:PCBM, P3HT:PCBM and PCPDTBT:PCBM solar cells under 1 sun white light illumination.

Photoactive layer	Type	J_{sc} (A m^{-2})	V_{oc} (V)	FF (%)	MPP (mW cm^{-2})
PF10TBT:PCBM	Conventional	67.3	0.96	61	4.0
	Inverted	66.1	0.95	59	3.7
P3HT:PCBM	Conventional	87.6	0.57	66	3.2
	Inverted	91.5	0.59	60	3.2
PCPDTBT:PCBM	Conventional	91.8	0.61	50	2.8
	Inverted	91.4	0.58	50	2.6

were obtained with variable angle spectroscopic ellipsometry [24,35]. The layer thicknesses of the ZnO and MoO_3 layers for this simulation have been defined as 20 and 10 nm, respectively. This was done to mimic the actual devices as closely as possible, and as such these thicknesses are not necessarily optimized for the optical field. As can be seen in Fig. 4, the calculated integrated exciton generation rates for both the conventional and inverted cells are equal to within 1% for the two structures. This validates the experimentally observed equal short-circuit currents under the assumption of equal internal quantum efficiencies. In this figure the origin is defined as the point in the photoactive layer where the light first enters the device,

i.e. the substrate side. For the conventional device the light is directly reflected at the aluminium top electrode, whereas for the inverted device the 10 nm of MoO_3 acts as an optical spacer, thereby changing the shape of the absorption envelope.

4. Conclusions

In summary, we have shown the electrical operation of inverted solar cells with an ITO/ZnO cathode, fabricated through the low temperature decomposition of $Zn(acac)_2$. The performance of these cells is shown to be equivalent to cells made in the conventional bottom-anode–top-cathode geometry. The simplicity of fabrication of these inverted solar cells without loss of performance will stimulate a further systematic investigation on their enhanced stability.

Acknowledgements

The authors thank J. Harkema and F. van der Horst for technical assistance. The work of P. de Bruyn was supported by the Dutch Polymer Institute (DPI), project DPI No. 660. The work of D.J.D. Moet was funded by SenterNovem via the EOS Long Term program ZOMER (EOS LT 03026).

References

[1] M.A. Green, K. Emery, Y. Hishikawa, W. Warta, Prog. Photovoltaics 17 (2009) 320.
[2] Y. Liang, Z. Xu, J. Xia, S. Tsai, Y. Wu, G. Li, C. Ray, L. Yu, Adv. Mater. 22 (2010) 1.
[3] M.P. de Jong, L.J. van IJzendoorn, M.J.A. de Voigt, Appl. Phys. Lett. 77 (2000) 2255.
[4] K.W. Wong, H.L. Yip, Y. Luo, K.Y. Wong, W.M. Lau, K.H. Low, H.F. Chow, Z.Q. Gao, W.L. Yeung, C.C. Chang, Appl. Phys. Lett. 80 (2002) 2788.
[5] C. Tao, S. Ruan, X. Zhang, G. Xie, L. Shen, X. Kong, W. Dong, C. Liu, W. Chen, Appl. Phys. Lett. 93 (2008) 193307.
[6] G. Li, C. Chu, V. Shrotriya, J. Huang, Y. Yang, Appl. Phys. Lett. 88 (2006) 253503.
[7] H. Liao, L. Chen, Z. Xu, G. Li, Y. Yang, Appl. Phys. Lett. 92 (2008) 173303.
[8] F.C. Krebs, Org. Electron. 10 (2009) 761.
[9] S.K. Hau, H.L. Yip, H. Ma, A.K.Y. Jen, Appl. Phys. Lett. 93 (2008) 233304.
[10] F.C. Krebs, Sol. Energy Mater. Sol. Cells 92 (2008) 715.
[11] A.K.K. Kyaw, X.W. Sun, C.Y. Jiang, G.Q. Lo, D.W. Zhao, D.L. Kwong, Appl. Phys. Lett. 93 (2008) 221107.
[12] J. Gilot, M.M. Wienk, R.A.J. Janssen, Appl. Phys. Lett. 90 (2007) 143512.
[13] D.J.D. Moet, L.J.A. Koster, B. de Boer, P.W.M. Blom, Chem. Mater. 19 (2007) 5856.
[14] W. Beek, M. Wienk, R. Janssen, Adv. Mater. 16 (2004) 1009.
[15] S.D. Oosterhout, M.M. Wienk, S.S. van Bavel, R. Thiedmann, L. Jan Anton Koster, J. Gilot, J. Loos, V. Schmidt, R.A.J. Janssen, Nat. Mater. 8 (2009) 818.
[16] C. Pacholski, A. Kornowski, H. Weller, Angew. Chem., Int. Ed. 41 (2002) 1188.
[17] T. Matsushima, Y. Kinoshita, H. Murata, Appl. Phys. Lett. 91 (2007) 253504.
[18] X. Jiang, Z. Zhang, J. Cao, W. Zhu, Solid-State Electron. 52 (2008) 952.
[19] H. You, Y. Dai, Z. Zhang, D. Ma, J. Appl. Phys. 101 (2007) 026105.
[20] H. Lee, S.W. Cho, K. Han, P.E. Jeon, C. Whang, K. Jeong, K. Cho, Y. Yi, Appl. Phys. Lett. 93 (2008) 043308.
[21] D.Y. Kim, J. Subbiah, G. Sarasqueta, F. So, H. Ding, Irfan, Y. Gao, Appl. Phys. Lett. 95 (2009) 093304.
[22] T. Arii, A. Kishi, J. Therm. Anal. Calorim. 83 (2006) 253.
[23] M. Morana, M. Wegscheider, A. Bonanni, N. Kopidakis, S. Shaheen, M. Scharber, Z. Zhu, D. Waller, R. Gaudiana, C. Brabec, Adv. Funct. Mater. 18 (2008) 1757.
[24] L.H. Slooff, S.C. Veenstra, J.M. Kroon, D.J.D. Moet, J. Sweelssen, M.M. Koetse, Appl. Phys. Lett. 90 (2007) 143506.
[25] M. Lenes, G.A.H. Wetzelaer, F.B. Kooistra, S.C. Veenstra, J.C. Hummelen, P.W.M. Blom, Adv. Mater. 20 (2008) 2116.
[26] F. Verbakel, S.C.J. Meskers, R.A.J. Janssen, Appl. Phys. Lett. 89 (2006) 102103.
[27] W.J.E. Beek, M.M. Wienk, M. Kemerink, X. Yang, R.A.J. Janssen, J. Phys. Chem. B 109 (2005) 9505.
[28] J. Peet, J.Y. Kim, N.E. Coates, W.L. Ma, D. Moses, A.J. Heeger, G.C. Bazan, Nat. Mater. 6 (2007) 497.
[29] J.M. Kroon, M.M. Wienk, W.J.H. Verhees, J.C. Hummelen, Thin Solid Films 403–404 (2002) 223.
[30] M. Lenes, M. Morana, C.J. Brabec, P.W.M. Blom, Adv. Funct. Mater. 19 (2009) 1106.
[31] J.D. Kotlarski, P.W.M. Blom, L.J.A. Koster, M. Lenes, L.H. Slooff, J. Appl. Phys. 103 (2008) 084502.
[32] L.A.A. Pettersson, L.S. Roman, O. Inganas, J. Appl. Phys. 86 (1999) 487.
[33] H. Hoppe, N. Arnold, D. Meissner, N.S. Sariciftci, Thin Solid Films 451–452 (2004) 589.
[34] N. Persson, H. Arwin, O. Inganas, J. Appl. Phys. 97 (2005) 034503.
[35] D.J.D. Moet, M. Lenes, J. Kotlarski, S. Veenstra, J. Sweelssen, M.M. Koetse, B. de Boer, P.W.M. Blom, Org. Electron. 10 (2009) 1275.